Assessing the validity of the thermodynamic uncertainty relation in quantum systems

Bijay Kumar Agarwalla[1] and Dvira Segal[2]

[1]*Department of Physics, Dr. Homi Bhabha Road, Indian Institute of Science Education and Research, Pune 411008, India*
[2]*Chemical Physics Theory Group, Department of Chemistry, and Centre for Quantum Information and Quantum Control, University of Toronto, 80 Saint George Street, Toronto, Ontario, Canada M5S 3H6*

(Received 19 June 2018; revised manuscript received 4 October 2018; published 26 October 2018)

We examine the so-called thermodynamic uncertainty relation (TUR), a cost-precision trade-off relationship in transport systems. Based on the fluctuation symmetry, we derive a condition for invalidating the TUR for general nonequilibrium (classical and quantum) systems. We find that the first nonzero contribution to the TUR beyond equilibrium, given in terms of nonlinear transport coefficients, can be positive or negative, thus affirming or violating the TUR depending on the details of the system. We exemplify our results for noninteracting quantum systems by expressing the thermodynamic uncertainty relation in the language of the transmission function. We demonstrate that quantum coherent systems that do not follow a population Markovian master equation, e.g., by supporting high-order tunneling processes or relying on coherences, violate the TUR.

DOI: 10.1103/PhysRevB.98.155438

I. INTRODUCTION

A thermodynamic uncertainty relation (TUR) describing a trade-off between entropy production (cost) and precision (noise) was recently derived for classical Markovian systems operating at steady state [1–5], with generalizations to finite-time [6], time-discrete, and driven Markov chains [7]. The thermodynamic uncertainty relation has generated significant research work directed at understanding its ramifications to dissipative systems such as biochemical motors and heat engines [8] and probing its validity in the classical regime [9–12] and beyond [13,14].

For a two-terminal single-affinity system, the TUR connects the steady-state averaged current $\langle j \rangle$, its variance $\langle\langle j^2 \rangle\rangle$, and the entropy production rate σ in a nonequilibrium process as

$$\frac{\langle\langle j^2\rangle\rangle}{\langle j\rangle^2}\frac{\sigma}{k_B} \geqslant 2. \tag{1}$$

This relation reduces to an equality in linear response: the current and the entropy production rate are linear in the thermodynamic affinity A, $\langle j \rangle = GAT$, (T is the temperature), $\sigma = \langle j \rangle A$, and the noise satisfies the fluctuation-dissipation relation with the linear transport coefficient G, $\langle\langle j^2 \rangle\rangle = 2Gk_BT$. Away from equilibrium, Eq. (1) points to a fundamental trade-off between precision and dissipation: A precise process with little noise is realized with a high thermodynamic (entropic) cost. We refer to systems that obey this inequality as "satisfying the TUR." TUR violations correspond to situations in which the left-hand side of Eq. (1) is smaller than 2.

Several interesting questions immediately come to mind when inspecting the TUR. Does it hold for other systems beyond Markov processes? Away from equilibrium, can we derive the TUR from fundamental principles, essentially from the fluctuation symmetry [15–19]? What is the role of quantum effects in validating or violating the inequality [13]? Recent studies addressed the potential of quantum coherences to reduce fluctuations in quantum heat engines [14].

The objective of our work is to understand the validity/invalidity of the TUR from fundamental principles beyond specific examples. In particular, (i) using the steady-state nonequilibrium fluctuation symmetry, we achieve a condition for violating the TUR, written as a series expansion in the applied bias voltage, and (ii) we study quantum systems that do not satisfy Markovian dynamics and rationalize violations of the TUR in certain regimes of operation.

We emphasize that multiaffinity systems such as thermoelectric junctions go above the lower bound of 2 even close to equilibrium [20], while a single-affinity system shows an equality in linear response. In this work, we focus our attention on the latter situation, where a far-from-equilibrium condition is necessary for departing from an equality in Eq. (1).

The paper is organized as follows. In Sec. II, we organize the TUR relationship in orders of applied voltage, while using the fundamental fluctuation symmetry. We analyze fermionic quantum transport junctions in Sec. III by deriving a closed-form condition on the TUR. We study examples in Sec. IV and conclude in Sec. V.

II. PERTURBATIVE ANALYSIS OF THE TUR FOLLOWING THE FLUCTUATION RELATION

The TUR was derived in Refs. [1–3] for classical Markov processes. Here, we arrive at a general connection between the current and its fluctuations for arbitrary systems, classical or quantum, by performing a perturbative expansion in the bias voltage and employing the nonequilibrium fluctuation symmetry. To the first nontrivial (second) order in voltage, the resulting combination can take values below 2, thus demonstrating a violation of the TUR.

The setup that we have in mind is a junction, where a finite-size system is sandwiched between two fermionic leads with a bias voltage V. The steady-state fluctuation symmetry [15–19], an outcome of the microreversibility principle of the underlying dynamics and the local detailed balance condition, relates the probability for transferring n carriers from high to low voltage over the time interval t, $P_t(n)$, to the probability of transferring charges against the applied voltage, $P_t(-n)$ (assuming $e=1$),

$$\ln\left[\frac{P_t(n)}{P_t(-n)}\right] = \beta V n, \tag{2}$$

where $\beta = 1/k_B T$ is the inverse temperature. We define the characteristic function, $\mathcal{Z}(\alpha) \equiv \langle e^{i\alpha n}\rangle = \sum_{n=-\infty}^{\infty} P_t(n) e^{i\alpha n}$, and the long-time limit of the cumulant-generating function (CGF) as $\chi(\alpha) = \lim_{t\to\infty} \frac{1}{t}\ln \mathcal{Z}(\alpha)$, or equivalently

$$\chi(\alpha) = \lim_{t\to\infty} \frac{1}{t} \sum_{p=1}^{\infty} \langle\langle n^p \rangle\rangle \frac{(i\alpha)^p}{p!}. \tag{3}$$

The steady-state fluctuation relation (2) dictates the symmetry $\chi(\alpha) = \chi(-\alpha + i\beta V)$. The fluctuation symmetry ensures relations between transport coefficients, specifically [17],

$$S_0 = 2\, k_B\, T\, G_1,$$
$$S_1 = k_B\, T\, G_2. \tag{4}$$

The first equation is the Johnson-Nyquist (fluctuation-dissipation) relation. The second equation uncovers a universal relation in the nonlinear transport regime, beyond the Onsager relation. Here, the steady-state charge current and its associated fluctuations (noise) are expanded in order of applied voltage,

$$\langle j \rangle = G_1 V + \frac{1}{2!} G_2 V^2 + \frac{1}{3!} G_3 V^3 + \cdots$$
$$\langle\langle j^2 \rangle\rangle = S_0 + S_1 V + \frac{1}{2!} S_2 V^2 + \frac{1}{3!} S_3 V^3 + \cdots. \tag{5}$$

Here, $G_1, G_2, G_3, \ldots$ are the linear and nonlinear transport coefficients. Similarly, $S_0, S_1, S_2, \ldots$ are the equilibrium and nonequilibrium noise terms. The associated entropy production is the joule's heating, $\sigma = V\langle j\rangle/T$.

We are now ready to put these relations together, and we find that

$$\beta V \frac{\langle\langle j^2\rangle\rangle}{\langle j\rangle} = \frac{\beta}{G_1} S_0 + \frac{\beta V}{G_1}\left[S_1 - \frac{S_0\, G_2}{2\, G_1}\right] + \frac{\beta V^2}{G_1} \times \left[\frac{S_2}{2} - \frac{S_0 G_3}{6 G_1} + \frac{S_0 G_2^2}{4 G_1^2} - \frac{S_1 G_2}{2 G_1}\right] + \mathcal{O}(V^3) + \cdots$$
$$= 2 + \frac{V^2}{G_1} C_{\rm neq} + \mathcal{O}(V^3) + \cdots, \tag{6}$$

where we define the combination $C_{\rm neq}$ as

$$C_{\rm neq} \equiv \frac{\beta}{6}[3S_2 - 2k_B T G_3]. \tag{7}$$

Note that the $\mathcal{O}(V)$ term disappears in the above expression precisely due to Eq. (4), an outcome of the nonequilibrium fluctuation symmetry (2).

Equations (6) and (7) are central results of this work: a combination of nonlinear transport coefficients determine the validity of the TUR. In the $\mathcal{O}(V^2)$, the TUR is satisfied to second order in voltage if $C_{\rm neq} \geqslant 0$. It is violated once $C_{\rm neq} < 0$. Equation (6) holds for arbitrary classical or quantum junctions. The only underlying requirement behind it are relationships (4) between transport coefficients, in and beyond linear response, which are grounded in the fluctuation relation. One can further extend this result for systems under a magnetic field and for bosonic systems. A nontrivial consequence of our work is that for Markov processes, high-order transport coefficients satisfy an inequality, $S_2 \geqslant \frac{2}{3} k_B T G_3$. The next section examines this derivation in quantum transport problems.

III. NONINTERACTING CHARGE TRANSPORT: FORMULA FOR THE TUR VIOLATION

We focus here on a generic noninteracting quantum charge transport problem and study the validity ($C_{\rm neq} \geqslant 0$) and breakdown ($C_{\rm neq} < 0$) of the TUR based on the perturbative expansion Eq. (6), as well as exact simulations. We consider a tight-binding chain connected to two fermionic leads that are maintained at different chemical potentials but at the same temperature. The steady-state cumulant-generating function associated with the integrated charge current was first derived by Levitov-Lesovik [21–23]. It was later extended to finite-size systems [24,25] and written following the Keldysh nonequilibrium Green's function formalism [15,26]. It is given by

$$\chi(\alpha) = \int_{-\infty}^{\infty} \frac{dE}{2\pi\hbar} \ln\big(1 + \mathcal{T}(E)\{f_L(E)[1 - f_R(E)](e^{i\alpha} - 1) + f_R(E)[1 - f_L(E)](e^{-i\alpha} - 1)\}\big). \tag{8}$$

Here, $\mathcal{T}(E)$ is the transmission function for charge transport at energy E. It can be calculated from the retarded and advanced Green's function of the system and from its self-energy matrix [27,28]. The transmission function is restricted to $0 \leqslant \mathcal{T}(E) \leqslant 1$. α is a counting parameter for charge transfer. $f_\nu(E) = [e^{\beta(E-\mu_\nu)} + 1]^{-1}$ is the Fermi distribution function for the two metal electrodes $\nu = L$ and R. As mentioned above, the CGF satisfies the steady-state fluctuation symmetry, $\chi(\alpha) = \chi(-\alpha + i\beta V)$, where $V = \mu_L - \mu_R$ [29]. From the CGF, one can generate all the cumulants. In particular, to interrogate the TUR we need to focus on the current and its fluctuations, given as $\langle j\rangle = \frac{\partial \chi}{\partial(i\alpha)}|_{\alpha=0}$ and $\langle\langle j^2\rangle\rangle = \frac{\partial^2\chi}{\partial(i\alpha)^2}|_{\alpha=0}$. Working out Eq. (8) we get

$$\langle j\rangle = \int_{-\infty}^{\infty} \frac{dE}{2\pi\hbar} \mathcal{T}(E)[f_L(E) - f_R(E)],$$
$$\langle\langle j^2\rangle\rangle = \int_{-\infty}^{\infty} \frac{dE}{2\pi\hbar}\big(\mathcal{T}(E)\{f_L(E)[1 - f_L(E)] + f_R(E)[1 - f_R(E)]\} + \mathcal{T}(E)[1 - \mathcal{T}(E)] \times [f_L(E) - f_R(E)]^2\big). \tag{9}$$

To test the TUR, we can use the exact expressions (9) in simulations. However, to gain a deeper understanding of this trade-off relationship we employ the voltage-perturbative expression (6). To find the nonequilibrium transport coefficients, we Taylor-expand the current and its noise in orders of V around equilibrium, $\mu_L = \mu + V/2$ and $\mu_R = \mu - V/2$, and get

$$G_3 = \frac{1}{4}\int_{-\infty}^{\infty} \frac{dE}{2\pi\hbar}\mathcal{T}(E)\frac{\partial^3 f(E)}{\partial\mu^3},$$
$$S_2 = 2\,k_B T\, G_3 + 2\int_{-\infty}^{\infty}\frac{dE}{2\pi\hbar}\mathcal{T}(E)[1-\mathcal{T}(E)]\left(\frac{\partial f(E)}{\partial\mu}\right)^2. \tag{10}$$

We proceed and simplify the third-order derivative using the following relation, $\partial^3 f/\partial\mu^3 + 6\beta(\partial f/\partial\mu)^2 = \beta^2\partial f/\partial\mu$. Below we also make use of the linear conductance,

$$G_1 = \int_{-\infty}^{\infty}\frac{dE}{2\pi\hbar}\mathcal{T}(E)\frac{\partial f(E)}{\partial\mu}. \tag{11}$$

Substituting the transport coefficients (10) into Eq. (7), we gather

$$\beta V\frac{\langle\langle j^2\rangle\rangle}{\langle j\rangle} = 2 + \frac{\beta^2 V^2}{6G_1}\int_{-\infty}^{\infty}\frac{dE}{2\pi\hbar}\mathcal{T}(E)\frac{\partial f(E)}{\partial\mu} \times\{1 - 6\mathcal{T}(E)f(E)[1-f(E)]\} + \mathcal{O}(V^3). \tag{12}$$

Here, $f(E)$ is the equilibrium Fermi function. Following Eq. (6) we identify $C_{\rm neq}$ by

$$C_{\rm neq} \equiv \frac{\beta^2}{6}\int_{-\infty}^{\infty}\frac{dE}{2\pi\hbar}\mathcal{T}(E)\frac{\partial f(E)}{\partial\mu} \times\{1-6\mathcal{T}(E)f(E)[1-f(E)]\}. \tag{13}$$

This function can switch sign depending on the structure of the transmission function and the contribution coming from the Fermi distribution. The validity of the TUR thus delicately depends on the properties of the system, i.e., its energetics and its coupling to the leads, hidden within the transmission function, as well as external conditions, i.e., the temperature.

Equation (13) is a central result of this work. Evaluating it gives a direct measure for TUR violation within second order in voltage. This expression can be furthermore supported by comparing its prediction to exact numerical results. We now discuss several limiting cases of this formula.

Low transmission, $\mathcal{T}(E) \ll 1$. The limit of small transmission corresponds to uncorrelated electron transfer processes. In Eq. (9), if we disregard the quadratic $[\mathcal{T}(E)]^2$ expression, assuming it is small relative to $\mathcal{T}(E)$, we find that the nonequilibrium noise always exceeds the equilibrium value. This limit, of a small transmission probability, should correspond to a Poisson statistics for transferred electrons, which is strongly linked to Markov processes. Specifically, in this limit Eq. (13) yields $\beta^2 G_1/6$, thus we get (up to V^2)

$$\beta V\frac{\langle\langle j^2\rangle\rangle}{\langle j\rangle} = 2 + \frac{\beta^2 V^2}{6}. \tag{14}$$

Since $C_{\rm neq} = \frac{\beta^2 G_1}{6} > 0$, the TUR is satisfied.

Constant transmission. If the transmission is a constant independent of energy, $\mathcal{T}(E) = \tau$, one can show that the TUR is satisfied. We note that $\beta f(1-f) = \frac{\partial f}{\partial\mu}$ and $G_1 = \frac{1}{2\pi\hbar}\tau$. We then perform the integration in Eq. (13) using $\int dE(\frac{\partial f}{\partial\mu}) = 1$ and $\frac{6}{\beta}\int dE(\frac{\partial f}{\partial\mu})^2 = 1$, and we obtain

$$\beta V\frac{\langle\langle j^2\rangle\rangle}{\langle j\rangle} = 2 + \frac{\beta^2 V^2}{12\pi\hbar G_1}\tau(1-\tau) \geqslant 2. \tag{15}$$

This result corresponds to the quantum limit of the TUR, with the thermal width of the Fermi distribution smaller than the broadening of resonances in the system. For low transmission values, we recover Eq. (14). For a perfect conductor or when approaching zero transmission, the TUR touches the lower (equilibrium) bound.

Resonance tunneling condition. We can greatly simplify Eq. (13) in the opposite limit, when the metal-system hybridization is weak. In this case, we assume that the transmission function is sharply peaked about a certain frequency, ϵ_d, which is set close to the Fermi energy, while the derivative of the Fermi function is relatively broad ($k_B T > \Gamma$). In this case, the principal contribution to the integral in Eq. (13) comes from the region near the resonance frequency ϵ_d. We can therefore replace the derivative of the Fermi function by a constant and simplify Eq. (13),

$$C_{\rm neq} = \frac{\beta^3}{6}f(\epsilon_d)[1-f(\epsilon_d)]\{\mathcal{T}_1 - 6f(\epsilon_d)[1-f(\epsilon_d)]\mathcal{T}_2\}, \tag{16}$$

where we define the integrals

$$\mathcal{T}_n \equiv \int_{-\infty}^{\infty}\frac{dE}{2\pi\hbar}\mathcal{T}^n(E). \tag{17}$$

Under this weak-coupling approximation, the violation of TUR ($C_{\rm neq} < 0$) translates into the inequality

$$\frac{\mathcal{T}_1}{\mathcal{T}_2} < 6f(\epsilon_d)[1-f(\epsilon_d)]. \tag{18}$$

Since $0 < f(1-f) < \frac{1}{4}$, the violation condition reduces to

$$\frac{\mathcal{T}_2}{\mathcal{T}_1} > \frac{2}{3}. \tag{19}$$

This inequality is another important result of our work. It should be pointed out that this condition for the violation of the TUR likewise holds for systems with multiple resonances ϵ_n, as long as these resonances are sharp and sufficiently close, $\epsilon_n, \Gamma_n < k_B T$, such that they are all positioned under the (approximately constant) envelope of $\frac{\partial f}{\partial\mu}$. Here, Γ is the characteristic width of the resonances.

IV. EXAMPLES

We illustrate the formal results of Sec. III within three central charge transport models: a single-dot resonant transmission model (A), a serial double-dot junction (B), and a side-coupled double-dot model (C). The three models are sketched in Fig. 1. As we demonstrate and rationalize in this section, the three models show violations of the TUR in certain regimes—when it is understood that the population dynamics deviates from Markovianity.

The transmission functions of the three models are described in the Appendix and displayed in Fig. 2. While model A depicts a simple resonant-Lorentzian structure, models B and C show quantum interference effects. In particular,

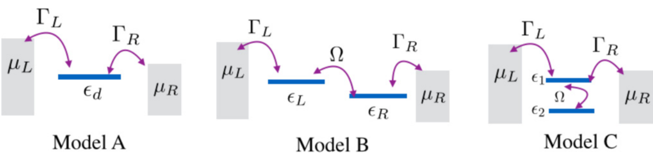

FIG. 1. Transport models that show violations of the TUR in different regimes: model A, a single-dot junction; model B, a serial double-dot junction; and model C, a side-coupled double-dot junction.

in model B, when Ω is small, the system includes two quasi degenerate levels (in the energy basis), and the transmission is suppressed at large Γ when both levels contribute. The side-coupled model C displays a node at $E=0$ due to a destructive interference effect; at large Γ, the transmission peak still reaches the unit value close to $E=0$, unlike model B. We note that the double-dot models B and C were recently analyzed in great detail for demonstrating destructive quantum interference effects in molecular electronic conduction [30–33].

Junctions A and B were recently studied in Ref. [14] based on the Levitov-Lesovik formula, as well as with a local Lindblad equation, manifesting TUR violations in different regimes. Our analysis in Secs. II and III lays out the theoretical groundwork for these curious observations and grants us a fundamental understanding of TUR violations.

In calculations below we position the equilibrium Fermi energy at $\mu=0$. Furthermore, for simplicity, we consider only symmetric junctions with identical hybridization energies, $\Gamma=\Gamma_{L,R}$. In simulations we compare analytical results, referring to the second order in the V formula, Eq. (12), to exact calculations using Eq. (9). For convenience, we also define the function

$$\mathcal{F} \equiv \beta V \frac{\langle\langle j^2\rangle\rangle}{\langle j\rangle} - 2, \tag{20}$$

where the breakdown of the TUR to any order in voltage corresponds to $\mathcal{F}<0$.

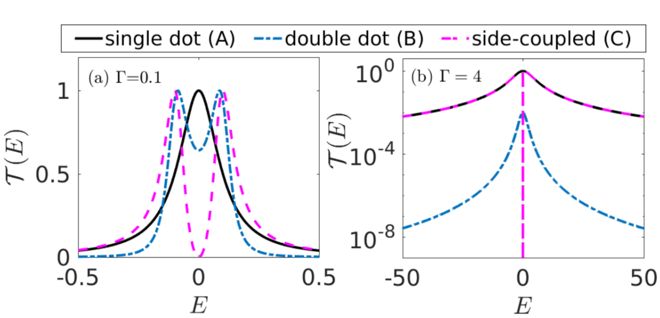

FIG. 2. Transmission functions for models A, B, and C at (a) weak and (b) strong couplings to the metal leads. Model A, single-dot junction: $\epsilon_d=0$. Model B, serial double-dot junction: $\epsilon_{L,R}=0$ and $\Omega=0.1$. Model C, side-coupled double-dot junction: $\epsilon_{1,2}=0$ and $\Omega=0.1$.

A. Model A: Single-dot junction

The junction includes a single site of energy ϵ_d coupled to two leads. The transmission function is given by

$$\mathcal{T}(E) = \frac{\Gamma_L\Gamma_R}{(E-\epsilon_d)^2+(\Gamma_L+\Gamma_R)^2/4}, \tag{21}$$

where we assume the wide-band limit for the spectral density of the baths, thus taking Γ as energy independent.

In the weak-coupling limit, the transmission function is sharply peaked around ϵ_d:

$$\mathcal{T}(E) = 2\pi\frac{\Gamma_L\Gamma_R}{\Gamma_L+\Gamma_R}\delta(E-\epsilon_d), \tag{22}$$

$$\mathcal{T}^2(E) = 4\pi\frac{\Gamma_L^2\Gamma_R^2}{(\Gamma_L+\Gamma_R)^3}\delta(E-\epsilon_d). \tag{23}$$

From here, we readily calculate the integrals $\mathcal{T}_1$ and $\mathcal{T}_2$, given as

$$\mathcal{T}_1 = \frac{1}{\hbar}\frac{\Gamma_L\Gamma_R}{\Gamma_L+\Gamma_R},$$
$$\mathcal{T}_2 = \frac{1}{\hbar}\frac{2\Gamma_L^2\Gamma_R^2}{(\Gamma_L+\Gamma_R)^3}. \tag{24}$$

Since $(\Gamma_L-\Gamma_R)^2 > -\Gamma_L\Gamma_R$, the condition in Eq. (19) cannot be satisfied and therefore the TUR is valid. In particular, when $\Gamma_L=\Gamma_R$, we find that $\mathcal{T}_2/\mathcal{T}_1=1/2$. In fact, this ratio is prevalent: systems with a set of sharp resonances show up this ratio at the weak-coupling limit.

In the very-strong-coupling regime, $\Gamma > \epsilon_d, k_BT$, we perform an asymptotic expansion with Γ, $\mathcal{T}(E)\sim 1-\frac{E^2}{\Gamma^2}+\frac{E^4}{\Gamma^4}$. We plug it into Eq. (13) and get

$$\beta V\frac{\langle\langle j^2\rangle\rangle}{\langle j\rangle} = 2+\frac{\beta^2V^2}{6}\left[\frac{a}{(\beta\Gamma)^2}+\frac{b}{(\beta\Gamma)^4}+\cdots\right], \tag{25}$$

where $a<0$ and $b>0$. Specifically, $a=(\pi^2/3-4)$ and $b=\frac{7\pi^4}{15}-18+\frac{\pi^2}{3}(\frac{\pi^2}{3}-4)$. Altogether, we find that for a single resonant level the TUR is satisfied at weak coupling when indeed the dynamics can be described by a Markovian population dynamics [34]. Nevertheless, it is violated at strong coupling when high-order tunneling processes contribute and the Markovian population dynamics breaks down [35]. In fact, under the V^2 expansion, the TUR is always violated at strong coupling in the single-dot model, with the function $C_{\rm neq}$ approaching zero from below.

In Fig. 3(a), we display the violation of the TUR in the single-dot model based on the analytical V^2 expansion, Eq. (12). We further compare simulations to the exact form, received from exact expressions for the current and noise, Eq. (9). We find that the quadratic formula (13) very well captures the deviation from linear response up to $\beta V\approx 1$. Figure 3(b) further shows that only at high voltage, $\beta V\gg 1$, when dissipation is excessive, is the TUR satisfied.

B. Model B: Serial double-dot junction

The serial double-dot junction includes two sites of energies ϵ_L and ϵ_R, which are coherently coupled to each other through the tunneling element Ω. The dots are individually coupled to the respective leads with dot ν coupled to the

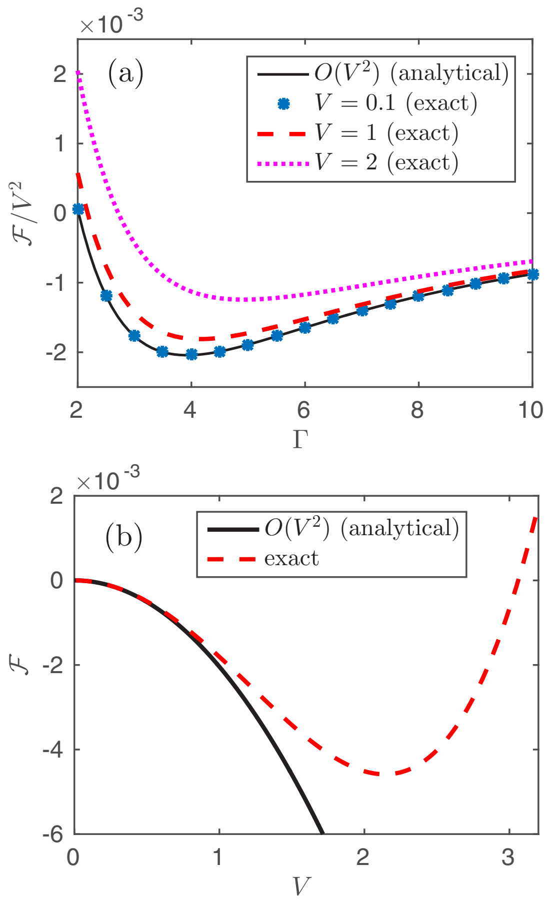

FIG. 3. Single quantum dot: Violation of the TUR ($\mathcal{F} < 0$), illustrated by varying the (a) metal-molecule coupling Γ and (b) voltage. Parameters are $\epsilon_d = 0$, $\beta = 1$, and $\Gamma = 4$ in panel (b). Exact calculations for $\mathcal{F}/V^2$ are based on Eq. (9). These are compared to the analytic formula (13); we display C_{neq}/G_1 in panel (a) and $V^2 C_{neq}/G_1$ in panel (b).

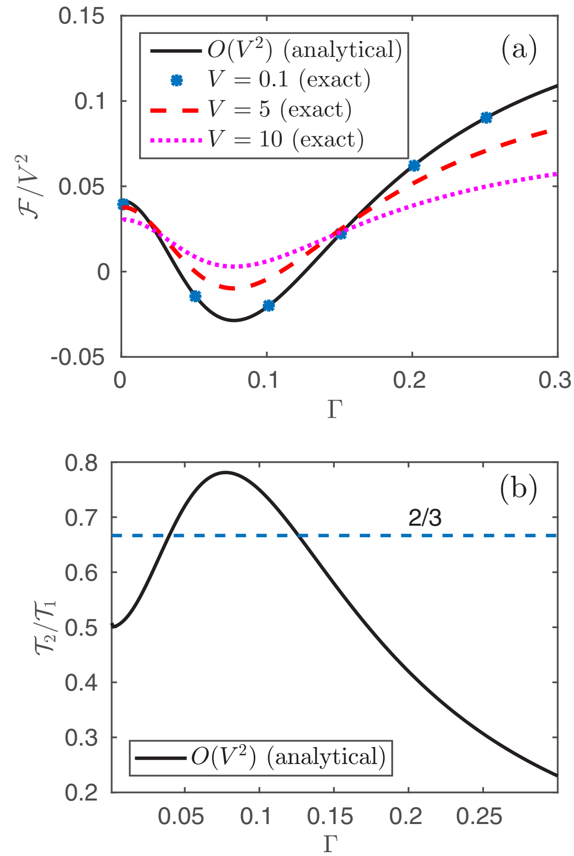

FIG. 4. Serial double quantum dot: (a) Violation of the TUR ($\mathcal{F} < 0$) within a certain range for Γ. The transmission function is given in Eq. (26), with $\epsilon_L = \epsilon_R = 0$, $\beta = 1$, $\Omega = 0.05$, and $\Gamma = 0.08$. Exact calculations for $\mathcal{F}/V^2$, based on Eq. (9), are compared to results from the analytic formula for C_{neq}/G_1 based on Eq. (13). (b) When the ratio $\mathcal{T}_2/\mathcal{T}_1$ (solid line) exceeds 2/3 (dashed line), the TUR is violated at weak coupling as shown in panel (a).

νth metal with the hybridization energy Γ_ν. The transmission function of a double dot is given by [14,33,36]

$$\mathcal{T}(E) = \frac{\Gamma_L \Gamma_R \Omega^2}{|(E - \epsilon_L + i\Gamma_L/2)(E - \epsilon_R + i\Gamma_R/2) - \Omega^2|^2}. \tag{26}$$

Assuming levels' degeneracy, $\epsilon_L = \epsilon_R$, a Markovian master equation neglecting coherences is generally inaccurate and cannot describe transport in this model even at weak coupling [34,37–40]. Thus, we expect TUR violations in this model when $\Gamma, \Omega < k_B T$. Under the symmetric coupling ($\Gamma_L = \Gamma_R = \Gamma$), we perform the integration (17) and obtain [14]

$$\mathcal{T}_1 = \frac{1}{\hbar} \frac{2\Gamma\Omega^2}{\Gamma^2 + 4\Omega^2},$$
$$\mathcal{T}_2 = \frac{1}{\hbar} \frac{4\Gamma\Omega^4(5\Gamma^2 + 4\Omega^2)}{(\Gamma^2 + 4\Omega^2)^3}. \tag{27}$$

According to Eq. (19), a violation of the TUR at weak coupling is expected when $\mathcal{T}_2/\mathcal{T}_1 > 2/3$, translated here as $4x^2 - 7x + 1 < 0$, with $x = \Omega^2/\Gamma^2$. This prediction is quite accurate as we find in Fig. 4.

In contrast, at strong coupling, $\Gamma \gg \Omega, k_B T$, the transmission function is suppressed because of a destructive interference effect [32,33,36]. In this limit the TUR is satisfied; recall that we proved in Eq. (14) that the TUR is valid when the transmission is small. We can also prove this result analytically. In the very-strong-coupling regime, $\Gamma \gg \Omega, k_B T$, an asymptotic expansion in Γ gives $\mathcal{T}(E) \sim 16\frac{\Omega^2}{\Gamma^2} + O(\frac{\Omega^4}{\Gamma^4})$. We plug this expansion into Eq. (13) and find that $C_{neq} > 0$ to order $1/\Gamma^2$.

We display our results for the double-dot model in Figs. 4 and 5. First, in Fig. 4(a) we show that the TUR can be violated at $\Gamma \sim \Omega$ and smaller that the thermal energy, specifically here in the range $0.04 < \Gamma < 0.126$. This observation agrees with Ref. [14]. We again confirm that Eq. (13) very well performs even at high voltage, compared to exact calculations from Eq. (9). We further verify in Fig. 4(b) that TUR violations take place precisely when $\mathcal{T}_2/\mathcal{T}_1 > 2/3$. This inequality thus serves as an excellent estimate of TUR breaking at weak coupling.

We uphold the quadratic approximation (13) in Fig. 5(a) by manifesting that it is valid up to $\beta V \sim 2$, whether or

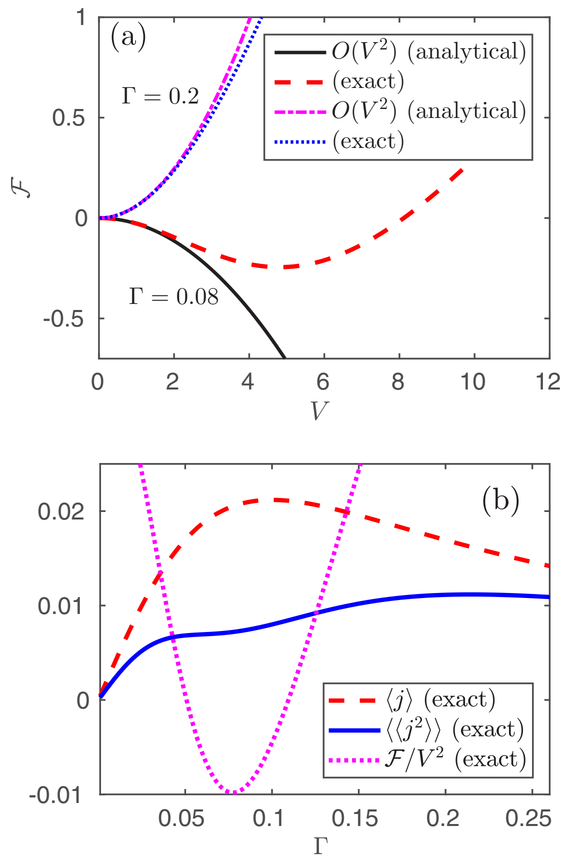

FIG. 5. Serial double quantum dot: (a) Violation of the TUR ($\mathcal{F} < 0$) as a function of bias. The transmission function, given in Eq. (26), is evaluated at $\epsilon_L = \epsilon_R = 0$, $\beta = 1$, and $\Omega = 0.05$. (b) The exact charge current $\langle j \rangle$, the associated noise $\langle\langle j^2 \rangle\rangle$, and the TUR function $\mathcal{F}/V^2$ plotted against Γ. Here $V = 5$. Other parameters are the same as those in panel (a).

not the TUR is verified. Finally, in Fig. 5(b) we display the players behind the TUR: the current and its fluctuations. The TUR is violated when the current is enhanced but the noise is suppressed, which is a favorable regime of operation.

C. Model C: Side-coupled double-dot junction

The side-coupled model includes two electronic sites of energies ϵ_1 and ϵ_2, where site 1 is directly coupled to the two metals and site 2 is side-coupled to site 1. Assuming the two sites are degenerate at the Fermi energy, $\epsilon_{1,2} = 0$, as we show in Fig. 2, the side-coupled junction displays a node at $E = 0$.

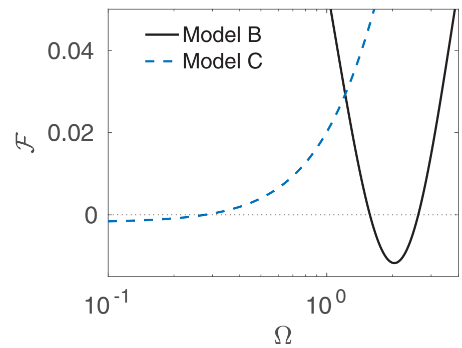

FIG. 6. Uncovering TUR violations in Model B ($\Omega/\Gamma \sim 1$) and Model C ($\Omega/\Gamma \ll 1$). We use $\beta = 1$, $V = 1$, and $\Gamma = 4$.

The transmission function of this model is given by

$$\mathcal{T}(E) = \frac{E^2 \Gamma_L \Gamma_R}{|[E + \frac{i}{2}(\Gamma_L + \Gamma_R)]E - \Omega^2|^2}. \quad (28)$$

At weak coupling $\Gamma < \Omega$, the transmission shows a two-peak structure around $\pm\Omega$. Given the node at $E = 0$, at very weak coupling we can approximate the transmission by two separate (close to) Lorentzian functions. We then conclude that similarly to the single-dot model, we precisely get $\mathcal{T}_2/\mathcal{T}_1 = 1/2$ when $\Gamma_L = \Gamma_R$. Therefore, according to Eq. (19), TUR violations are not expected at weak coupling in the side-coupled model. In contrast, at large couplings, $\Gamma \gg \Omega$, the transmission behaves similarly to the single-dot resonant level model A; therefore we expect to overturn the TUR. This could be rationalized by the breakdown of a Markovian master equation for population dynamics in this regime, due to the contribution of high-order tunneling processes [41,42]. Figure 6 displays TUR violations in models B and C using the complete expressions (9). It is significant to note that the models behave in a strikingly different way at weak and large splitting Ω/Γ.

We summarize our findings on the validity of the TUR for the single-dot, serial double-dot, and side-coupled double-quantum-dot setups in Table I. Here, validation of the TUR refers to satisfying the inequality to quadratic order in V.

V. SUMMARY

We investigated the validity of the thermodynamic uncertainty relation in a single-affinity junction beyond linear response. Based on the nonequilibrium fluctuation symmetry, we put together a relation among the current, its noise, and the entropy production, given in terms of nonlinear transport coefficients. From this relation we received a general condition for validating the TUR to second order in biasing/invalidating

TABLE I. Thermodynamic uncertainty relation for charge transport in quantum dot setups.

Hybridization Γ	Single-dot (A) and side-coupled (C) models	Serial double-dot model (B)
Weak	Valid $\mathcal{O}(V^2)$ (Markovian master equation for population)	Invalid (Non-Markovian population dynamics)
Strong	Invalid (High-order electron tunneling processes)	Valid $\mathcal{O}(V^2)$ (Low-transmission function)

it, Eqs. (6) and (7). This condition holds for both classical and quantum systems. We exemplified the analysis on an analytically tractable noninteracting fermionic system. We derived a general relation for invalidating the TUR, which was given in the language of the transmission function [Eq. (13)], and tested it with central charge transport models, with single and double (serial and side-coupled) quantum dots.

Future work will be focused on the exploration of the TUR in interacting (electron-electron and electron-phonon) quantum systems based on analytical results for the cumulant-generating function [43] and on the analysis of parallel relations for heat-conducting systems [44]. Furthermore, we plan to study nonreciprocating continuous quantum heat machines that rely on quantum coherences for operation, e.g., absorption refrigerators [45–47], and search for optimized regimes of operation with suppressed fluctuations and high-output power.

ACKNOWLEDGMENTS

D.S. acknowledges support from the Natural Sciences and Engineering Research Council of Canada (NSERC) Discovery Grant and the Canada Research Chair Program. B.K.A. gratefully acknowledges the start-up funding from IISER Pune and the hospitality of the Department of Chemistry at the University of Toronto.

APPENDIX: TRANSMISSION FUNCTIONS

The transmission function that appears in the Levitov-Lesovik formula, Eq. (8), can be computed from the Green's function of the system and the self-energies resulting from its couplings to the leads:

$$\mathcal{T}(E) = \mathrm{Tr}[\hat{G}_0^r(E)\hat{\Gamma}_L(E)\hat{G}_0^a(E)\hat{\Gamma}_R(E)]. \tag{A1}$$

Here, $\hat{G}_0^{r,a}(E)$ is the retarded (advanced) Green's function for the system and $\hat{\Gamma}_{L,R}$ are the hybridization matrices that include the coupling to the reservoirs (electrodes) L and R.

Model A. The single-dot model, also referred to as the resonant transmission model, includes a single electronic level with a site energy, ϵ_d, which is coupled to two leads. In this case, the Green's functions are c-numbers, $G_0^r(E) = [E - \epsilon_d + i(\Gamma_L(E) + \Gamma_R(E))/2]^{-1}$ and $G_0^a(E) = [G_0^r(E)]^\dagger$. In general, the hybridization parameter depends on energy, $\Gamma(E)$. Nevertheless, for simplicity, in the main text we use a wide-band model with a fixed value for Γ. The transmission function is given by

$$\mathcal{T}(E) = \frac{\Gamma_L(E)\Gamma_R(E)}{(E - \epsilon_d)^2 + [\Gamma_L(E) + \Gamma_R(E)]^2/4}, \tag{A2}$$

reducing to Eq. (21) in the wide-band limit.

Model B. The serial double-quantum-dot setup comprises two levels with site energies ϵ_L and ϵ_R. The dots are coupled to each other with a coherent tunneling, Ω. Each dot is furthermore coupled to its respective metal lead. The Green's functions of the system are 2×2 matrices, given by

$$\hat{G}_0^r(E) = \{E\hat{I} - \hat{H}_S - [\hat{\Sigma}_L^r(E) + \hat{\Sigma}_R^r(E)]\}^{-1}, \tag{A3}$$

where the system Hamiltonian is

$$\hat{H}_S = \begin{bmatrix} \epsilon_L & \Omega \\ \Omega & \epsilon_R \end{bmatrix}, \tag{A4}$$

with $\hat{\Sigma}_L(E) = -\frac{i}{2}\hat{\Gamma}_L(E)$, and similarly for $\hat{\Sigma}_R(E)$. The self-energy matrices are

$$\hat{\Gamma}_L(E) = \begin{bmatrix} \Gamma_L(E) & 0 \\ 0 & 0 \end{bmatrix}, \quad \hat{\Gamma}_R(E) = \begin{bmatrix} 0 & 0 \\ 0 & \Gamma_R(E) \end{bmatrix}. \tag{A5}$$

The resulting transmission function is

$$\mathcal{T}(E) = \frac{\Gamma_L(E)\Gamma_R(E)\Omega^2}{|[E - \epsilon_L + i\Gamma_L(E)/2][E - \epsilon_R + i\Gamma_R(E)/2] - \Omega^2|^2}. \tag{A6}$$

In the wide-band limit we acquire Eq. (26).

Model C. The side-coupled model includes two dots of energies ϵ_1 and ϵ_2, which are coherently coupled. In this design, level 1 is coupled to both metal leads while level 2 does not directly connect to the electrodes. The system Hamiltonian $\hat{H}_S$ and the matrix $\hat{\Gamma}_L(E)$ are given by Eqs. (A4) and (A5). Since level 1 couples to both leads, $\hat{\Gamma}_R(E)$ is given by

$$\hat{\Gamma}_R(E) = \begin{bmatrix} \Gamma_R(E) & 0 \\ 0 & 0 \end{bmatrix}. \tag{A7}$$

Gathering the transmission function we get

$$\mathcal{T}(E) = \frac{(E - \epsilon_2)^2\Gamma_L(E)\Gamma_R(E)}{|\{E - \epsilon_1 + \frac{i}{2}[\Gamma_L(E) + \Gamma_R(E)]\}(E - \epsilon_2) - \Omega^2|^2}. \tag{A8}$$

Using $\epsilon_{1,2} = 0$, we find that the transmission shows a node at $E = 0$ and a double-peak structure at $E = \pm\Omega$.

[1] A. C. Barato and U. Seifert, Thermodynamic Uncertainty Relation for Biomolecular Processes, Phys. Rev. Lett. **114**, 158101 (2015).

[2] P. Pietzonka, A. C. Barato, and U. Seifert, Universal bounds on current fluctuations, Phys. Rev. E **93**, 052145 (2016).

[3] T. R. Gingrich, J. M. Horowitz, N. Perunov, and J. L. England, Dissipation Bounds All Steady-State Current Fluctuations, Phys. Rev. Lett. **116**, 120601 (2016).

[4] J. M. Horowitz and T. R. Gingrich, Proof of the finite-time thermodynamic uncertainty relation for steady-state currents, Phys. Rev. E **96**, 020103(R) (2017).

[5] P. Pietzonka and U. Seifert, Universal Trade-Off between Power, Efficiency, and Constancy in Steady-State Heat Engines, Phys. Rev. Lett. **120**, 190602 (2018).

[6] P. Pietzonka, F. Ritort, and U. Seifert, Finite-time generalization of the thermodynamic uncertainty relation, Phys. Rev. E **96**, 012101 (2017).

[7] K. Proesmans and C. Van den Broeck, Discrete-time thermodynamic uncertainty relation, Europhys. Lett. **119**, 20001 (2017).

[8] R. Marsland III, and J. England, Limits of predictions in thermodynamic systems: A review, Rep. Prog. Phys. **81**, 016601 (2018).

[9] C. Hyeon and W. Hwang, Physical insight into the thermodynamic uncertainty relation using Brownian motion in tilted periodic potentials, Phys. Rev. E **96**, 012156 (2017).

[10] A. Dechant and S. Sasa, Current fluctuations and transport efficiency for general Langevin systems, J. Stat. Mech.: Theory Exp. (2018) 063209.

[11] V. Holubec and A. Ryabov, Cycling Tames Power Fluctuations near Optimum Efficiency, Phys. Rev. Lett. **121**, 120601 (2018).

[12] T. Koyuk, U. Seifert, and P. Pietzonka, A generalization of the thermodynamic uncertainty, arXiv:1809.02113.

[13] K. Brandner, T. Hanazato, and K. Saito, Thermodynamic Bounds on Precision in Ballistic Multiterminal Transport, Phys. Rev. Lett. **120**, 090601 (2018).

[14] K. Ptaszynski, Coherence-enhanced constancy of a quantum thermoelectric generator, Phys. Rev. B **98**, 085425 (2018).

[15] M. Esposito, U. Harbola, and S. Mukamel, Nonequilibrium fluctuations, fluctuation theorems, and counting statistics in quantum systems, Rev. Mod. Phys. **81**, 1665 (2009).

[16] M. Campisi, P. Hänggi, and P. Talkner, Colloquium: Quantum fluctuation relations: Foundations and applications, Rev. Mod. Phys. **83**, 771 (2011).

[17] K. Saito and Y. Utsumi, Symmetry in full counting statistics, fluctuation theorem, and relations among nonlinear transport coefficients in the presence of a magnetic field, Phys. Rev. B **78**, 115429 (2008).

[18] U. Seifert, Stochastic thermodynamics, fluctuation theorems, and molecular machines, Rep. Prog. Phys. **75**, 126001 (2012).

[19] D. Andrieux, P. Gaspard, T. Monnai, and S. Tasaki, The fluctuation theorem for currents in open quantum systems, New. J. Phys. **11**, 043014 (2009).

[20] K. Macieszczak, K. Brandner, and J. P. Garrahan, Unified thermodynamic uncertainty relations in linear response, Phys. Rev. Lett. **121**, 130601 (2018).

[21] L. S. Levitov and G. B. Lesovik, Charge distribution in quantum shot noise, Pis'ma Zh. Eksp. Teor. Fiz. **58**, 225 (1993) [JETP Lett. **58**, 230 (1993)].

[22] L. S. Levitov, H.-W. Lee, and G. B. Lesovik, Electron counting statistics and coherent states of electric current, J. Math. Phys. **37**, 4845 (1996).

[23] I. Klich, in *Quantum Noise in Mesoscopic Physics*, NATO Science Series II, Vol. 97, edited by Yu. V. Nazarov (Kluwer, Dordrecht, 2003).

[24] K. Schönhammer, Full counting statistics for noninteracting fermions: Exact results and the Levitov-Lesovik formula, Phys. Rev. B **75**, 205329 (2007).

[25] K. Schönhammer, Full counting statistics for noninteracting fermions: Exact finite-temperature results and generalized long-time approximation, J. Phys.: Condens. Matter **21**, 495306 (2009).

[26] B. K. Agarwalla, B. Li, and J.-S. Wang, Full-counting statistics of heat transport in harmonic junctions: Transient, steady states, and fluctuation theoremsPhys. Rev. E **85**, 051142 (2012).

[27] A. Nitzan, *Chemical Dynamics in Condensed Phases: Relaxation, Transfer and Reactions in Condensed Molecular Systems* (Oxford University, London, England, 2006).

[28] M. Di Ventra, *Electrical Transport in Nanoscale Systems* (Cambridge University, Cambridge, England, 2008).

[29] G. Gallavotti and E. G. D. Cohen, Dynamical Ensembles in Nonequilibrium Statistical Mechanics, Phys. Rev. Lett. **74**, 2694 (1995).

[30] C. R. Arroyo, S. Tarkuc, R. Frisenda, J. S. Seldenthuis, C. H. M. Woerde, R. Eelkema, F. C. Grozema, and H. S. J. van der Zant, Signatures of quantum interference effects on charge transport through a single Benzene ring, Angew. Chem. **125**, 3234 (2013).

[31] V. Rabache, J. Chaste, P. Petit, M. L. Della Rocca, P. Martin, J.-C. Lacroix, R. L. McCreery, and P. Lafarge, Direct observation of large quantum interference effect in anthraquinone solid-state junctions, J. Am. Chem. Soc. **135**, 10218 (2013).

[32] T. Markussen and K. S. Thygesen, Temperature effects on quantum interference in molecular junctions, Phys. Rev. B **89**, 085420 (2014).

[33] R. Hartle, M. Butzin, and M. Thoss, Vibrationally induced decoherence in single-molecule junctions, Phys. Rev. B **87**, 085422 (2013).

[34] S. A. Gurvitz and Ya. S. Prager, Microscopic derivation of rate equations for quantum transport, Phys. Rev. B **53**, 15932 (1996).

[35] C. Emary, Counting statistics of cotunneling electrons, Phys. Rev. B **80**, 235306 (2009).

[36] L. Simine, W. J. Chen, and D. Segal, Can Seebeck coefficient identify quantum interference in molecular conduction? J. Phys. Chem. C **119**, 12097 (2015).

[37] J. Aghassi, A. Thielmann, M. H. Hettler, and G. Schön, Shot noise in transport through two coherent strongly coupled quantum dots, Phys. Rev. B **73**, 195323 (2006).

[38] U. Harbola, M. Esposito, and S. Mukamel, Quantum master equation for electron transport through quantum dots and single molecules, Phys. Rev. B **74**, 235309 (2006).

[39] G. Schaller, G. Kieshlich, and T. Brandes, Transport statistics of interacting double dot systems: Coherent and non-Markovian effects, Phys. Rev. B **80**, 245107 (2009).

[40] C. Flindt, T. Novotny, A. Braggio, and A.-P. Jauho, Counting statistics of transport through Coulomb blockade nanostructures: High-order cumulants and non-Markovian effects, Phys. Rev. B **82**, 155407 (2010).

[41] I. Djurica, B. Dong, and H. L. Cui, Super-Poissonian shot noise in the resonant tunneling due to coupling with a localized level, Appl. Phys. Lett. **87**, 032105 (2005).

[42] H.-B. Xue, Full counting statistics as a probe of quantum coherence in a side-coupled double quantum dot system, Ann. Phys. **339**, 208 (2013).

[43] B. K. Agarwalla, J.-H. Jiang, and D. Segal, Full counting statistics of vibrationally assisted electronic conduction: Transport and fluctuations of thermoelectric efficiency, Phys. Rev. B **92**, 245418 (2015).

[44] K. Saito and A. Dhar, Fluctuation Theorem in Quantum Heat Conduction, Phys. Rev. Lett. **99**, 180601 (2007).

[45] R. Kosloff and A. Levy, Quantum heat engines and refrigerators: Continuous devices, Annu. Rev. Phys. Chem. **65**, 365 (2014).

[46] M. Kilgour and D. Segal, Coherence and decoherence in quantum absorption refrigerators, Phys. Rev. E **98**, 012117 (2018).

[47] V. Holubec and T. Novotny, Effects of noise-induced coherence on the performance of quantum absorption refrigerators, J. Low Temp. Phys. **192**, 147 (2018).